

## Aerodynamics of Nanjing Tower: A case study

Ahsan Kareem<sup>a,\*</sup>, Scott Kabat<sup>a</sup>, Fred L. Haan Jr.<sup>b</sup>

<sup>a</sup>*NatHaz Modeling Laboratory, Department of Civil Engineering and Geological Sciences,  
University of Notre Dame, 163 Fitzpatrick, Notre Dame, IN 46556-0767, USA*

<sup>b</sup>*Department of Aerospace and Mechanical Engineering, University of Notre Dame,  
163 Fitzpatrick, Notre Dame, IN 46556-0767, USA*

---

### Abstract

Numerical simulations and experimental measurements of the aerodynamics of the Nanjing Tower have been conducted. The tower consists of three legs of rectangular cross section that support an observation deck at 180 m elevation, a circular shaft which supports another deck at 240 m, and a structure of square cross section extending to the tower's highest point of 310 m. Aerodynamic forces on the tower were numerically derived by dividing the tower into various basic shapes and synthesizing available experimental data for these shapes into mode-generalized forces – an aerodynamic building block approach. A boundary layer wind tunnel experiment was also conducted using a high-frequency force balance and a lightweight tower model. Similar values resulted from these numerical and experimental studies. The tower response in both alongwind and acrosswind directions was evaluated. © 1998 Elsevier Science Ltd. All rights reserved.

---

### 1. Introduction

This paper addresses the aerodynamics of TV towers with particular reference to the 310 m Nanjing Tower in Nanjing, PRC. Active/passive dampers (i.e. active mass driver and tuned liquid dampers) are currently being designed for installation on the Nanjing Tower under US/PRC guidance to improve its performance under wind and seismic loads. Completed in May 1993, the VIP lounge may experience wind induced accelerations greater than human comfort levels during wind events exceeding a threshold value. The tower's structural integrity is not in question; rather, it may

---

\*Corresponding author. E-mail: kareem@navier.ce.nd.edu.

experience motion levels that may exceed PRC’s regulations for human comfort. The effectiveness of these devices will be assessed through full-scale monitoring of the tower. This structure will serve as a testbed for future performance evaluation of motion control devices. The first author is participating in this project with the following objectives: (1) response analysis under wind in the presence and absence of control devices, (2) development and design of tuned liquid dampers; and (3) field testing and performance evaluation of control systems. This paper deals with the aerodynamics of the Nanjing Tower. Other investigators include: Drs. T.T. Soong, A.M. Reinhorn, J.N. Yang, M. Shinozuka, D.A. Reed and M. Feng [1].

TV towers have a distinct structural profile consisting of several structural shapes, e.g. circular observation decks and support systems with vertical or flared legs. Such a configuration often makes these structures sensitive to the dynamic action of wind. Some TV towers have circular cylindrical shapes with variable diameters along the height, e.g. Hornigsprinde and Munich towers in Germany. Others typically have three long supporting legs with observation decks and antenna masts stacked above these. The geometry and layout of these legs can have profound influence on the aerodynamics of these towers. Nanjing Tower in Nanjing, China [2], CN Tower in Toronto [3], and Stratosphere in Las Vegas [4], are three examples of the latter class of tower structural system.

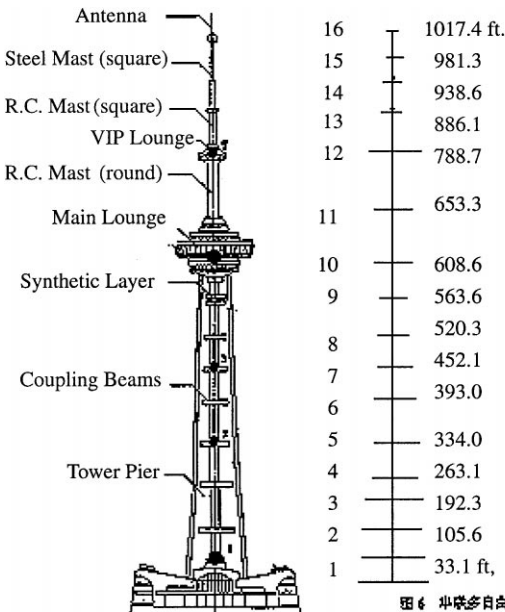


图 6 华塔多自由度图

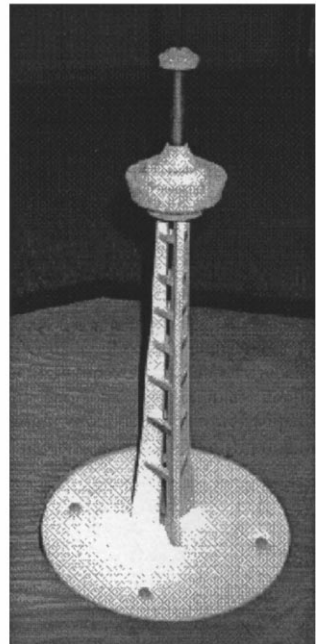


Fig. 1. The Nanjing Tower – actual system with 16 degrees of freedom and wind tunnel model.

The Nanjing Tower's (Fig. 1) profile is similar to the CN Tower in Toronto and the Stratosphere in Las Vegas, but has some peculiar aerodynamic features. All the three towers are supported by three legs of rectangular cross sections of varying depth arranged symmetrically about the center. The CN Tower has a central shaft that connects all three legs throughout the height and makes it a bluff configuration, whereas the Stratosphere has arc-shaped legs with a central shaft which results in openings between the legs near the bottom and the top. Nanjing Tower does not have a central shaft (elevators run through the tower legs) which creates a continuous opening between the legs except for some interference by cross-beams introduced for stability. This configuration makes Nanjing Tower aerodynamically efficient since openings are known to introduce beneficial effects. Nanjing Tower has a large, revolving skypod (observation deck) at a height of 180 m and a small, fixed skypod at a height of 240 m. Both decks have a circular shape with diameter varying with height. A circular shaft connects the two decks and a structure of square cross section extends above the small deck.

Like other tall, flexible structures, TV towers are sensitive to the buffeting action of turbulence in the alongwind direction and wake excitation in the acrosswind direction. The acrosswind excitation is very much dependent on the tower profile and particularly on the continuity in the profile geometry. For example, a continuous circular section tower will experience more coherent vortex shedding action as opposed to a tower with distinct structural components jutting out. Some of these protruding elements may have the effect of disrupting the coherence of the vortex excitation. The observation decks, often circular in cross section, are less vulnerable to organized vortex shedding due to their stubby configuration, i.e. their small height to diameter ratio, and their variable diameter along the height. Wind blowing over the top and bottom of such structural elements tends to preclude the formation of a coherent vortex shedding pattern.

Besides the overall structural stability, wind induced effects strongly influence a tower's serviceability. Occupants of observation decks or revolving restaurants located in TV towers can experience discomfort during wind events. Telecommunication dishes and antennas are also affected by large excursions of the tower from its undisturbed position.

In this study, the alongwind and acrosswind loading spectra are derived by drawing from past experience in wind tunnel studies dealing with tower-shaped structures and from computational recipes based on a synthesis of experimental data for various shapes which constitute the tower structure. The tower was essentially divided into three basic shapes, namely, circular, square, and triangular. Although the leg configuration is not exactly a triangular cross section due to the opening, a closed section was assumed to provide a conservative estimate. The acrosswind spectral description was synthesized by a covariance integration scheme. In the alongwind direction, a simple buffeting model based on quasi-steady and strip theories was used to derive mode-generalized spectra. A wind tunnel study using a high-frequency force balance was conducted to validate predictive techniques used in the above aerodynamic building block-type study. Also, a parametric study was performed in the wind tunnel to observe the influence of closing the gap between the tower legs.

### 2. Dynamic response analysis

Both alongwind and acrosswind response were evaluated in the frequency domain, whereas the alongwind response was also analyzed in the time domain. Common to both response calculations is a random vibration-based approach to compute system rms response. The system's equation of motion in modal coordinates is given by

$$m_i \ddot{y}_i + 2m_i \omega_i \zeta_i \dot{y}_i + k_i y_i = \phi_i^T F(t) \tag{1}$$

in which  $m_i$ ,  $\zeta_i$ ,  $k_i$ ,  $\omega_i$ , and  $\phi_i$  are the  $i$ th modal mass, damping, stiffness, frequency, and mode shape, respectively.

The mass and stiffness matrices for the Nanjing Tower are provided in Ref. [1]. From these parameters, natural frequencies and mode shapes were determined (Fig. 2). The first mode damping ratio was set at 2%, and damping ratios for higher modes were calculated using the following relation [5,6]:

$$\zeta_i = \zeta_1 \left( 1 + 0.38 \left( \frac{f_i}{f_1} - 1 \right) \right) \tag{2}$$

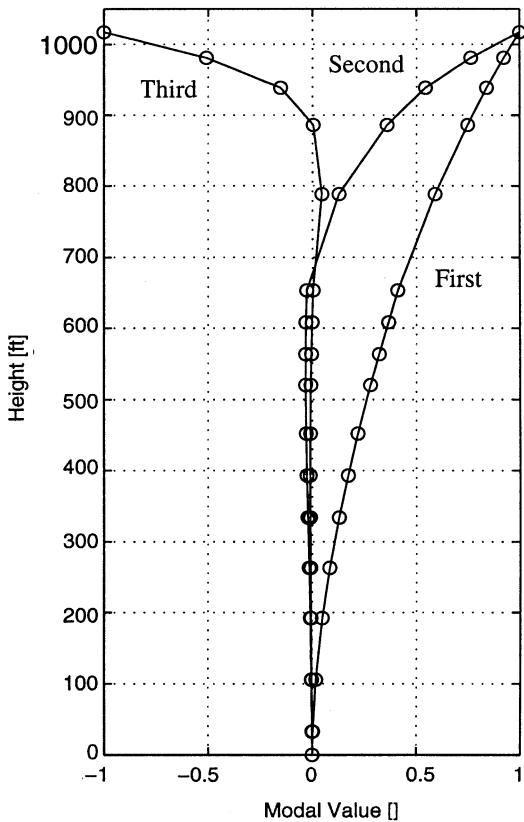


Fig. 2. Mode shapes.

The mean-square value of the acceleration response is the area under the spectral density function

$$\sigma_{\ddot{y}_i}^2 = \int_{-\infty}^{\infty} |H(f)|^2 S_F(f) df. \quad (3)$$

For lightly damped structures, the integral can be simplified by replacing the forcing function with a white noise equal to the value of  $S_F(f)$  at the natural frequency of interest [7]. Using this approximation, Eq. (3) can be rewritten as

$$\sigma_{\ddot{y}_i}^2 = \frac{\pi S_F^i(f_i) f_i}{4\zeta_i m_i^2}, \quad (4)$$

where  $S_F^i(f_i)$  is the spectral density for the  $i$ th mode at the  $i$ th natural frequency. The contribution of the  $i$ th mode to the overall rms tower response in physical coordinates is given by

$$\sigma_{\ddot{x}_i}(z) = \phi_i(z) \sqrt{\frac{\pi f_i S_F^i(f_i)}{4\zeta_i m_i^2}}, \quad (5)$$

where  $\phi_i(z)$  is the modal value at the level of the lounge and  $x$  the response in physical coordinates [6].

### 3. Aerodynamic loading

The information provided in Ref. [1] concerning the Nanjing Tower is given for a 16 degree-of-freedom system. Some of the salient features are provided in Table 1. The analysis of the tower began by dividing the tower shape into 16 segments, each with a representative section width and height. For this study, the lower nine segments of the tower can be approximated by a triangular cross section. The wind was assumed to be perpendicular to any face of the triangle. The 10–12 sections were circular segments comprised of the two lounges and the cylindrical support between them. The antenna support was modeled as a square cross section for the final four segments.

In order to determine  $S_F^i(f_i)$ , the spectral density must be determined for each level and then converted to modal coordinates through multiplication by the appropriate modal vectors.

#### 3.1. Alongwind loading

The alongwind loading can be formulated based on strip and quasi-steady theories. Details can be found elsewhere in one of the author's previous studies [8], only the

Table 1  
Building parameters

No	Height (ft)	Mass (slugs × 10 <sup>-5</sup> )	Width (ft)	Area (ft <sup>2</sup> × 10 <sup>-3</sup> )	C <sub>d</sub>
1	33.1	2.73	104.6	3.47	1.4
2	105.6	4.92	95.9	6.95	1.4
3	192.2	6.85	82.8	7.17	1.4
4	263.1	8.43	78.4	5.56	1.4
5	334.0	9.75	74.1	5.25	1.4
6	393.0	10.86	69.7	4.12	1.4
7	452.1	11.97	65.4	3.86	1.4
8	520.3	12.88	61.0	4.16	1.4
9	563.6	15.20	56.6	2.45	1.4
10	608.6	19.09	122.0	5.48	0.8
11	653.5	20.13	21.8	0.98	0.8
12	788.7	20.99	52.3	7.07	0.8
13	886.2	21.01	11.5	1.11	1.0
14	938.6	21.111	5.9	0.31	1.0
15	981.2	21.121	3.6	0.15	1.0
16	1017.4	21.123	2.5	0.09	1.0

final expressions are given here:

$$S_F^{ii}(f) = \frac{4\bar{F}_i^2 S_u^i(f)}{\bar{U}^2} J_h^i(f) J_v^i(f), \tag{6}$$

$$S_F^{ij}(f) = \sqrt{S_F^i(f) S_F^j(f)} \text{coh}_{ij}(f), \tag{7}$$

$$\bar{F}_i = \rho C_{D_i} A_i U_i^2, \tag{8}$$

$$S_u^i(f) = \frac{4\chi(f)^2 \kappa \bar{U}^2}{f(2 + \chi(f)^2)^{4/3}}, \tag{9}$$

where  $S_F^i(f)$  is the spectral density at the  $i$ th level,  $\bar{F}_i$  the mean force at that level, and  $S_u^i(f)$  is the spectrum of the wind at the  $i$ th level. The description of the remaining quantities is given below:

$$\text{coh}_{ij}(f) = \exp\left(-10f \left| \frac{h_i - h_j}{0.5(U_i + U_j)} \right| \right), \tag{10}$$

$$J_h^i(f) = \frac{2}{(\gamma_y^i(f) C_h)^2} (e^{-(\gamma_y^i C_h)} + \gamma_y^i C_h - 1), \tag{11}$$

$$J_v^i(f) = \frac{2}{(\gamma_z^i(f) C_v)^2} (e^{-(\gamma_z^i C_v)} + \gamma_z^i C_v - 1), \tag{12}$$

$$\gamma_z^i(f) = \frac{2f\theta_i b_i}{U_i}, \quad \gamma_y^i(f) = \frac{2f\theta_i h_{S_i}}{U_i}, \quad \theta_i = \frac{\sqrt{1 + (r_i)^2}}{1 + r_i}, \tag{13}$$

$$r_i = \frac{C_h b_i}{C_v h_{S_i}}, \quad \chi(f) = \frac{4000f}{\bar{U}}, \tag{14}$$

where  $h_i$ ,  $C_{D_i}$ ,  $h_{S_i}$ ,  $U_i$ , and  $u_i$  are the section elevation above the ground, drag coefficient, section height, mean wind velocity, and fluctuating wind velocity, respectively;  $C_h$  and  $C_v$  are the horizontal and vertical separation factors, set at 8 and 10, respectively;  $\rho$  is the density of air,  $\kappa$  is set at 0.01, and  $\bar{U}$  is the wind velocity at 33 ft. According to the PRC Design Standard, the 10 year maximum wind based on the statistics at the site is equal to 60.0 ft/s at 10 m height. Wind velocities at any height in the boundary layer can be determined using the power law with a coefficient of 0.16. The fluctuating wind velocity and associated force field were digitally generated based on the prescribed spectral description. This program utilizes random phase and amplitude using an FFT approach to match the prescribed spectral description given above [9]. For validation purposes, the spectral results obtained from the preceding formulation can be compared with the results obtained from wind tunnel tests. These results are given in Fig. 9 and will be discussed in the wind tunnel section of this paper.

### 3.2. Acrosswind loading

Unlike the alongwind response for a structure, the acrosswind response cannot be determined using quasi-steady and strip theories. The response depends on the interaction of incident turbulence, unsteady wake effects, and, in some cases, on structural motion which cannot be described in a functional relationship to the incoming flow field characteristics [7]. While experimental research work has been focused on generic structures with typically uniform cross sections, the different shape components that appear in the Nanjing Tower cannot be fully quantified without a wind tunnel test of the Tower.

Before proceeding with a wind tunnel test, we wished to explore the potential of a “building block approach” in which the overall spectral description of the tower could be derived from its components with available aerodynamic loading descriptions. The spectral density for the acrosswind response for each section was determined from the experimentally derived spectra for each cross section. These plots are generally available in a non-dimensional form [10]. The  $x$ -axis values are reduced frequencies  $(fb)/U$  where  $b$  is a section width while  $y$ -axis values are a reduced spectral density based on a function of frequency, section width, height, and wind velocity. The velocity used for each segment corresponded to that at the top of the segment using the power law previously described.

For each section and appropriate spectra, the non-dimensionalized frequency was multiplied by velocity and divided by the section width. These frequency values,  $f^i$ , were then used to determine spectral density via:

$$S_F^i(f) = y^i / f^i (0.5 \rho b_i h_{S_i} U_i^2)^2, \quad (15)$$

where  $y^i$  are the non-dimensionalized spectral values for the  $i$ th section. In order to establish the cross-spectral relationship between different levels, an approximate coherence relationship was used based on the author's previous work [10]. In addition, for the triangular and square sections, each spectral density value had to be

adjusted since the given non-dimensional plots had been previously weighted to a linear mode shape. Since each segment has different frequency values, a linear interpolation scheme was used to determine spectral density values over the entire range of frequencies. The change in frequency was made very small to adequately model the peaks in the spectral data. As with the alongwind results, the comparison between the simulation results and those from the wind tunnel experiment are given in Fig. 10 in the experimental analysis portion of this paper.

The contributions of each section for the first three modes are shown in Fig. 3. Though the total contribution of the triangular cross sections has a very high peak at 0.15 Hz, the frequency content drops considerably after that and the value at the first natural frequency is only 18% of the maximum. The majority of the spectral contribution results from the circular cross sections that comprise the lounges. In fact, when compared to the total acrosswind loading spectrum of the tower, these sections contribute almost all of the energy in the first mode at the first natural frequency. However, in the second and third modes, it is the spectral contribution of the square antenna that contributes to the spectral energy near the natural second and third mode frequencies.

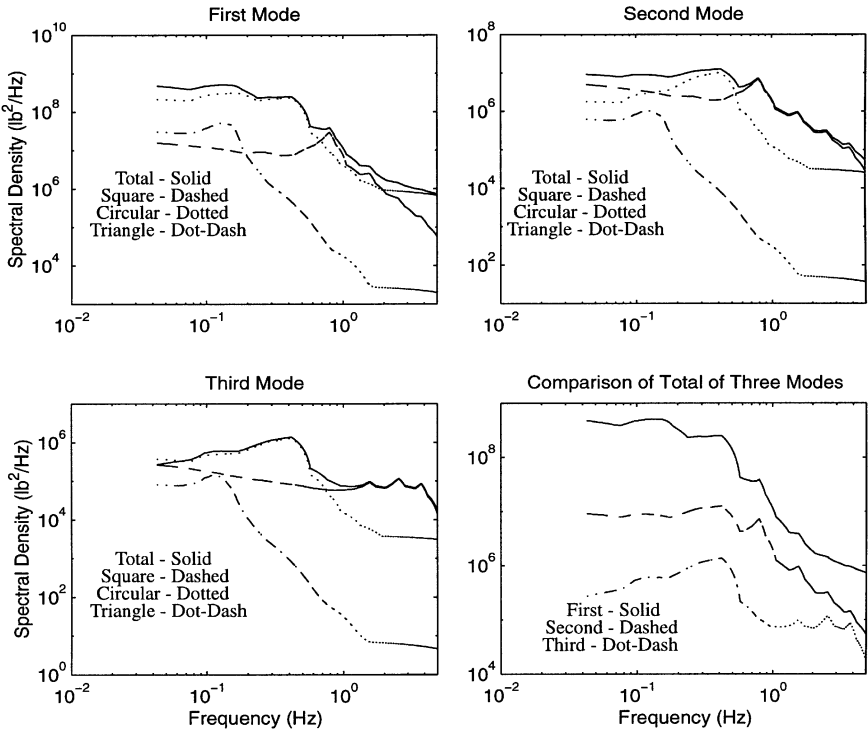


Fig. 3. Spectral contributions of tower sections to the acrosswind force spectra.

#### 4. Alongwind and acrosswind response

The results of the frequency-domain response analysis of the alongwind response for the first three modes are given in Table 2. The modal masses are determined from the data concerning the mass distribution in Table 1 and the mode shapes shown in Fig. 2. The time-domain response for each mode is given in Table 3. To determine response statistics in the time domain, several realizations of response time history were obtained, each using a different set of correlated wind velocities. The time and frequency results show a good agreement. A sample set of simulated wind velocities and the resulting acceleration for three sections of the tower is given in Fig. 4. It is interesting to note the high response amplitude of the mast above the VIP lounge.

The results of the acrosswind response estimates are given in Table 4 for the first three modes. Except for the spectral density values at the natural frequencies, all other values needed to determine the root-mean-square acceleration response from Eq. (5) are the same as those in Table 2. While it is uncommon for the structural response to have a relatively large contribution from the second mode, part of the reason is due to the decrease in modal mass from the first mode and the sensitivity of the square antenna support to the higher frequency response. As can be seen in Table 1 and Fig. 2, the high stiffness of the triangular section in the second and third mode results in a smaller modal mass. This combined with high contribution of the square cross section to the spectral description of the acrosswind loading in higher modes results in a relatively large component of response in the second and third modes in comparison with the fundamental mode.

Table 2  
Alongwind rms acceleration response for first three modes at VIP lounge in frequency domain

	1st	2nd	3rd
$f$ (Hz)	0.198	0.623	1.255
$S_f(f_i)$ (lbf <sup>2</sup> )	$5.45 \times 10^7$	$6.71 \times 10^4$	$1.17 \times 10^3$
$\zeta$ ( )	0.02	0.0363	0.0606
$m_i$ (slugs]	$1.51 \times 10^5$	$5.07 \times 10^3$	752
$\phi$ ( )	0.590	0.126	0.045
$\sigma$ (mg)	2.50	0.74	0.25

Table 3  
Alongwind rms acceleration response for first three modes at VIP lounge in time domain

Mode	Response (mg)
1	2.71
2	0.83
3	0.27

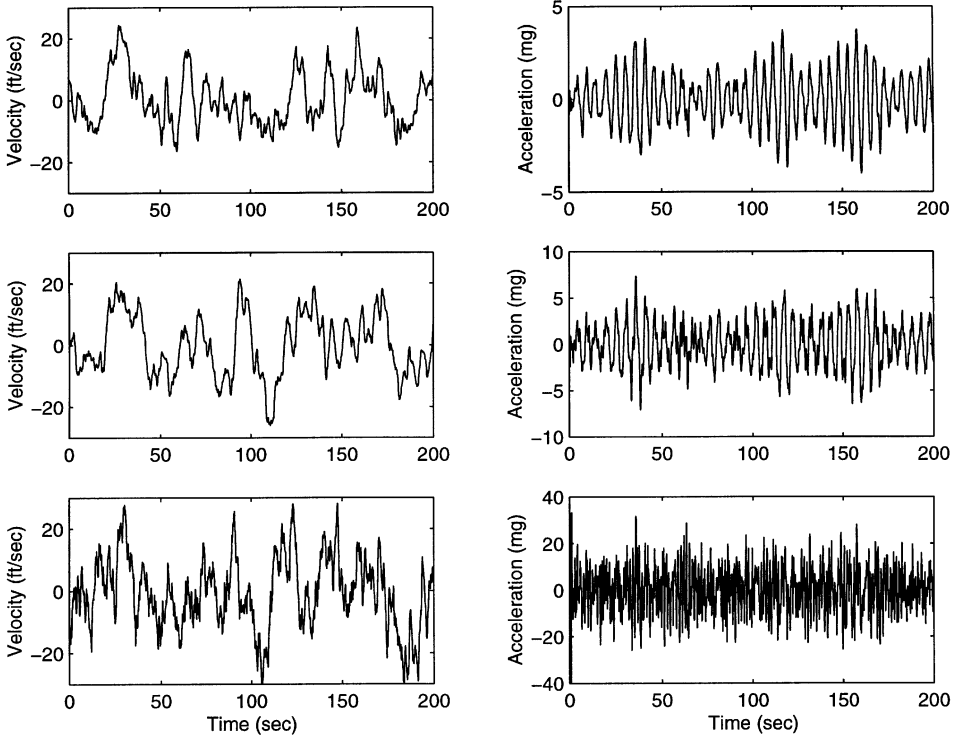


Fig. 4. Time histories and acceleration for three levels of tower from top to bottom wind velocities and accelerations at the main lounge, VIP lounge, and centre of square section mast.

Table 4  
Crosswind rms acceleration response for the VIP lounge for first three modes in frequency domain

Mode	$S_F(f_i)$ (lbf <sup>2</sup> )	Response (mg)
1	$3.31 \times 10^8$	6.19
2	$4.39 \times 10^6$	5.95
3	$7.52 \times 10^4$	2.04

### 5. Experimental analysis

To validate the predictive techniques described above and to observe the effects of closing the gap between the tower legs, an experimental study was conducted in the boundary layer wind tunnel, NatHaz Laboratory, Hessert Center for Aerospace Research, University of Notre Dame. In the 5 ft × 5 ft × 49 ft working section, spires complemented by surface roughness elements were employed to generate a boundary

layer with a power-law exponent of 0.16 to match site measurements. The Nanjing Tower itself was modeled by constructing a 22.25 in replica of balsa wood and styrofoam (see Fig. 1). A high-frequency force balance mounted beneath the tunnel floor returned voltages which were digitized and converted to overturning moment measurements with a PC-based data acquisition system. Assuming a fundamental mode shape that varies linearly with height, the generalized forces in the fundamental modes are proportional to these overturning moments. Measurements were made with the tower configured with gaps between its legs – like the actual tower – and without gaps. For the cases without gaps, masking tape was carefully applied to the model to cover the gaps without significantly violating the geometric integrity of the shape of the rest of the model. Two wind directions were considered: one case for one tower leg facing directly into the wind and one case rotated 180° from that configuration. These two cases are referred to here as one leg forward and two legs forward, respectively.

Figs. 5–8 show the results of the test cases. In each figure, power spectral density plots are shown for moment measurements with and without a gap through the tower legs. The alongwind case for two legs forward shows a slightly greater overall variance than that for one leg forward. And in each leg configuration, closing the gap has the effect of increasing the variance. Both the acrosswind configurations, however, show a significant increase in the low-frequency response for the closed gap cases over the open gap cases. In addition, having two legs forward with the gap closed showed a broad peak in the acrosswind response around 20–30 Hz which was not nearly so evident with the gap open. Clearly, the gap between the legs which allows the freestream fluid to increase base pressure plays an important role in the development of aerodynamic forces on the tower.

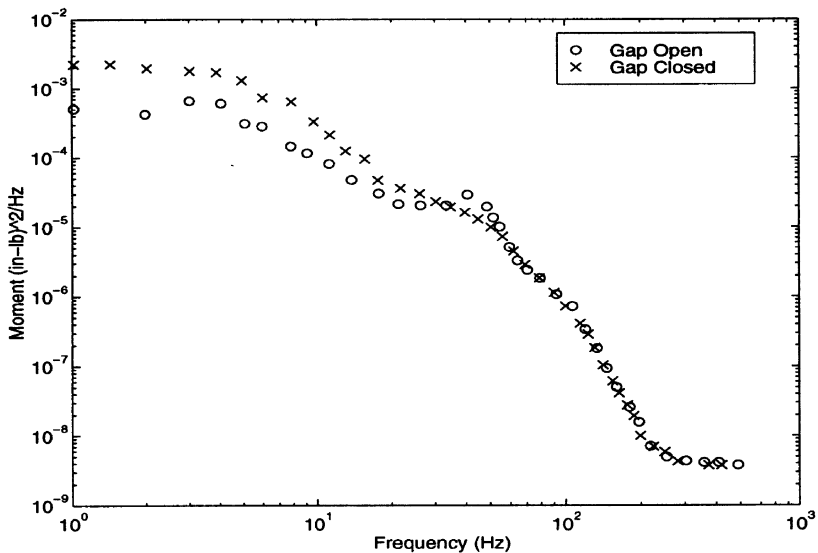


Fig. 5. Test case results for acrosswind moment one leg forward.

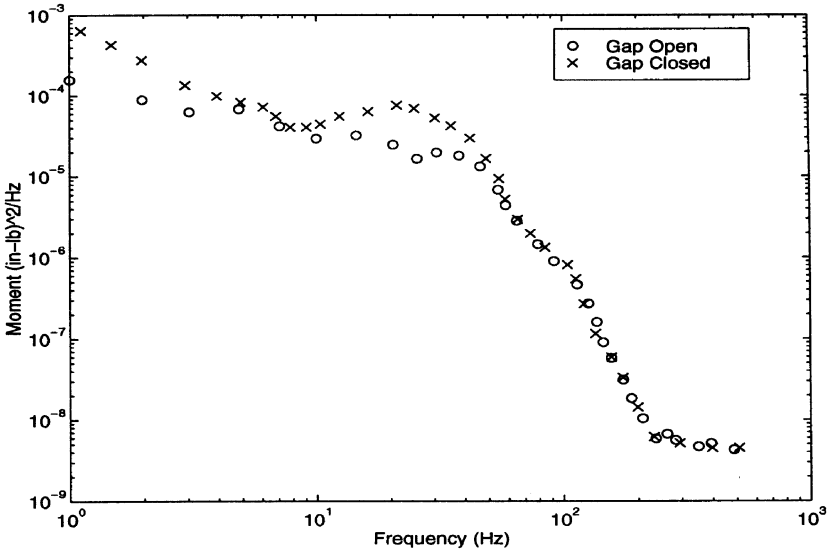


Fig. 6. Test case results for acrosswind moment two legs forward.

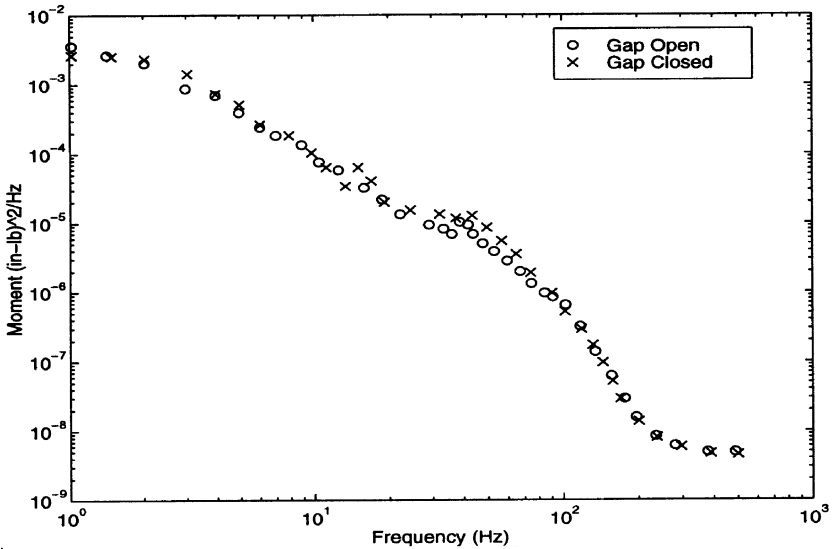


Fig. 7. Test case results for alongwind moment one leg forward.

Figs. 9 and 10 show the comparison between the simulation and the experimental results for the alongwind and acrosswind reactions. The wind tunnel results corresponded to those with two legs forward and the gaps between the legs closed. The additional line for the wind tunnel represents the actual results multiplied by 0.8 to

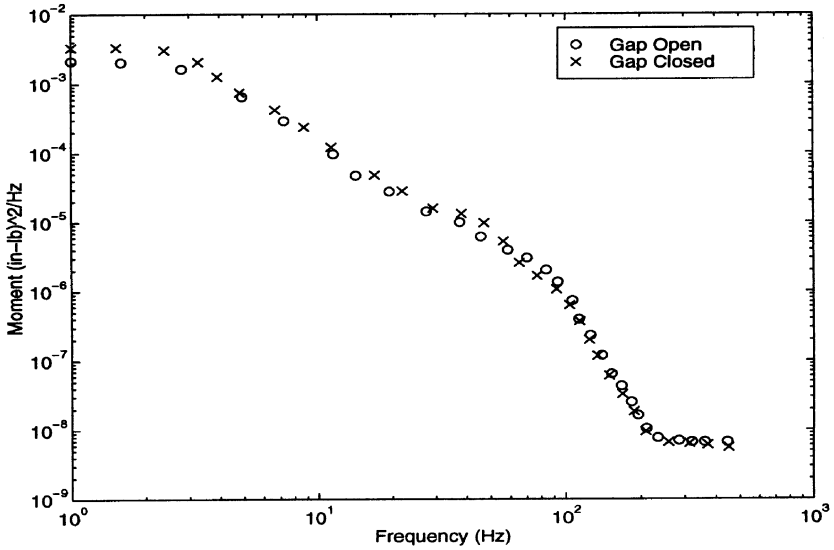


Fig. 8. Test case results for alongwind moment two legs forward.

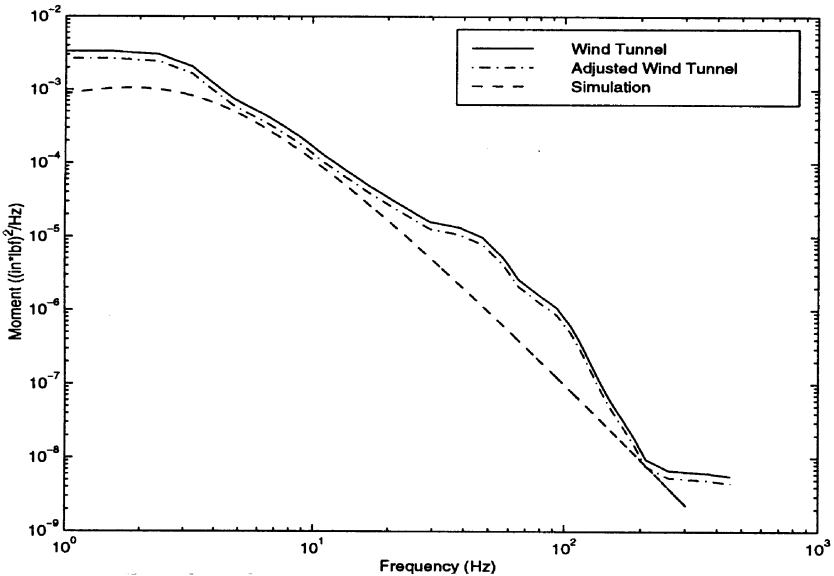


Fig. 9. Alongwind moment wind tunnel and simulation comparison.

adjust for the mode shape of the tower which departs from a linear shape implied in the force balance test. The results show a good comparison. For the acrosswind direction, some departure at high frequencies was noted which does not influence the response significantly.

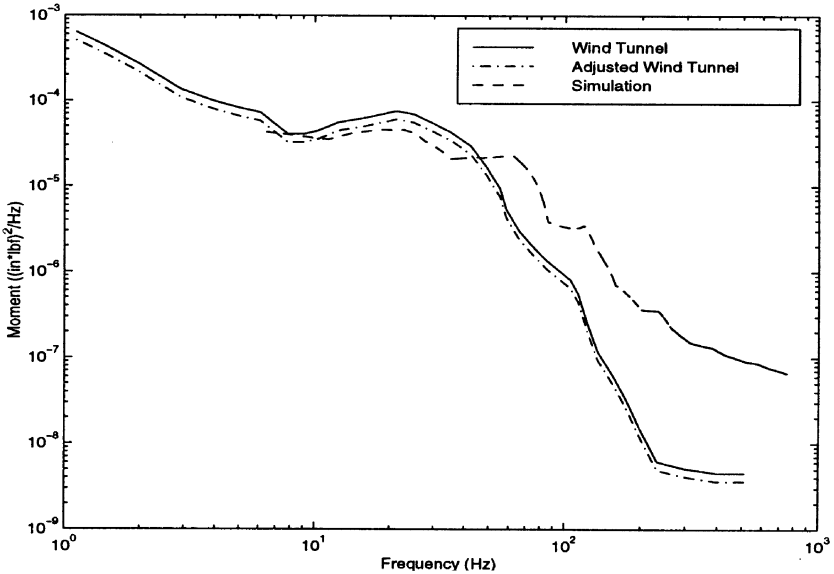


Fig. 10. Acrosswind moment wind tunnel and simulation comparison.

## 6. Conclusions

Aerodynamic loads and associated response of the Nanjing Tower based on quasi-steady and strip theories, the “aerodynamic building-block” method, and an experimental approach using a boundary layer wind tunnel are presented. Quasi-steady and strip theories were employed to formulate alongwind loadings in the time and frequency domains. Utilizing experimental aerodynamic data for basic geometric shapes, the mode-generalized forces on the tower were derived. A force-balance method was then employed in the wind tunnel to obtain fundamental-mode forces which compared very well with the computational results. The tower alongwind and acrosswind response was computed which exceeds human comfort thresholds. This has led to the development of an active mass driver to control the tower response. The experimental program also included a study of the effects of the gap between the tower’s legs. Closing this gap had little effect on the alongwind response while it significantly increased the acrosswind response.

## Acknowledgements

The support for this work was provided in part by the National Science Foundation Grants CMS-94-02196&CMS-95-03779. Their support is gratefully acknowledged.

**References**

- [1] A.M. Reinhorn, T.T. Soong, H. Cao, Design of active tuned mass damper for nanjing tower, US/PRC Cooperation Program, 28 September 1995.
- [2] D. Dajun, R. Zenhua, Design testing and analyses of Nanjing TV Tower, *Concrete Int.* 16 (11) (1994) 42–44.
- [3] J. Monbaliu, P.G. Dance, N. Isyumov, A.G. Davenport, Properties of the atmospheric boundary layer measure at the CN-Tower, Toronto, Canada, Proc. 5th USNCWE, Lubbock, TX, 1995.
- [4] Stratosphere Web Site – <http://www.klas-tv.com/stratosphere/>.
- [5] A. Kareem, Damping in structures: its evaluation and treatment of uncertainty, *J. Wind Eng. Ind. Aerodyn.* 59 (1996) 131–157.
- [6] A. Kareem, Wind excited response of buildings in higher modes, *J. Struct. Div. ASCE* 107 (ST4) Paper 16155 (1981) 701–706.
- [7] A. Kareem, Acrosswind response of buildings, *ASCE, J. Struct. Div.* 108 (1982) 869–887.
- [8] Y. Li, A. Kareem, Recursive modelling of dynamic systems, *J. Eng. Mech. ASCE* 116 (3) (1990) 660–679.
- [9] Y. Li, A. Kareem, Simulation of multivariate random processes: hybrid DFT and digital filtering approach, *J. Eng. Mech. ASCE* 119 (5) (1993) 1078–1098.
- [10] A. Kareem, Measurements of pressure and force fields on building models in simulated atmospheric flows, *J. Wind Eng. Ind. Aerodyn.* 36 (1990) 589–599.